Int J Clin Exp Med 2016;9(1):131-139
www.ijcem.com /ISSN:1940-5901/IJCEM0015471

Original Article

Magnetic resonance diffusion-weighted imaging and computed tomography in the diagnosis of hemangioma and venous malformations of head and neck among children

Guilun Yang[1], Jingxia Kang[1], Ming Zhu[2], Shoujiang Wang[1]

[1]Department of Medical Imaging, Linyi People's Hospital Affiliated to Shandong University, Linyi 276000, P. R. China; [2]Department of Medical Imaging, Traditional Chinese Medicine Hospital, Linyi 276000, P. R. China

Received September 1, 2015; Accepted December 5, 2015; Epub January 15, 2016; Published January 30, 2016

Abstract: Objective: To compare the diagnostic value between magnetic resonance diffusion-weighted imaging (MR-DWI) and computed tomography (CT) for hemangioma and venous malformations of head and neck among children. Methods: A total of 55 subjects were systematically recruited into this study, including 25 cases diagnosed with hemangioma and 30 cases with venous malformation. Diagnostic test was applied to evaluate accuracy, sensitivity and specificity of MR-DWI and CT in hemangioma and venous malformation, and Kappa test was further performed; independent sample t-test was adopted to compare ADC values between two groups. And receiver operating characteristic (ROC) curve was drawn for the optimal threshold in identification. Results: MR-DWI had higher sensitivity, specificity, accuracy, positive and negative predictive values than CT in diagnosing hemangioma and venous malformation. Both methods corresponded to clinicopathological analysis, and MR-DWI (K = 0.781) had significantly higher matching coefficient than CT (K = 0.566). When b = 500 s/mm^2, ADC value of venous malformation group was significantly higher than that of hemangioma group (P < 0.05); area under the ROC curve (AUC) diagnosed by MR-DWI was 0.924, and threshold was ADC = 1.615 × 10^{-3} mm^2/s, with sensitivity and specificity of 84.00% and 86.70%, respectively. When b = 1000 s/mm^2, similar pattern of ADC values in both groups was observed; AUC was 0.924, and threshold was ADC = 0.894 × 10^{-3} mm^2/s, showing sensitivity and specificity of 76.0% and 67.0%, respectively, which were lower compared with values obtained when b = 500 s/mm^2. Conclusion: MR-DWI had higher sensitivity, specificity, accuracy, positive and negative predictive values, and matching coefficient than CT for hemangioma and venous malformation diagnosis.

Keywords: MR-DWI, CT, hemangioma, venous malformation, diagnostic efficiency, matching coefficient, ADC value, b value

Introduction

Hemangioma is one of the most common benign tumors among children, but its aetiological factors remain unclear now, which was previously reported to be closely related to genetic factors [1]. Hemangioma begins with angiectasis, punctate red papules and red spots, with cyanosis on skin surface [1, 2]. About 1 year after birth, these symptoms will gradually disappear, leaving no trace [3]. However, this sort of hemangioma may lead to various secondary injuries such as anabrosis, infection, compressive and obstructive injury, and visceral injury, thus cannot be ignored [4]. Venous malformation, a symptom of congenital local cerebrovascular variability, has a low diagnostic rate in the early stage. Mainly characterized by intracranial hemorrhage, venous malformation has the occurrence rate of about 38%-70%, including a death rate of infantile hemorrhage of 10% [5], and may easily result in migraine, intracranial infection, and even fatal intracranial hemorrhage [6]. Therefore, it is of great significance to explore early diagnosis and efficacious treatment to both diseases.

Magnetic resonance imaging diffusion-weighted imaging (MR-DWI) is a common method in clinical diagnosis, which can produce contrast

Table 1. General pathological data of patients

	Hemangioma group (n = 25)	Venous malformation group (n = 30)	t/χ^2	*P*
Sex (male/female)	10/15	18/12	2.183	0.140
Age	2.68 ± 1.435	10.23 ± 5.14	7.107	< 0.001
Lesion extent (cm^2)	64.28 ± 44.97	68.70 ± 43.09	0.371	0.712
Pathogenic site				
Tempus	2	2		
Parotidean and masseteric region	5	8		
Cheeks	5	6	1.743	0.883
Lips	6	4		
Tongue and floor of mouth	3	6		
Neck	4	4		
Lesion color				
Cyanosis	16	18	0.092	0.761
Red	9	12		
Treatment means				
Interventional treatment of local embolism	15	17	0.062	0.803
Operative treatment	10	13		

MR-DWI: magnetic resonance diffusion-weighted imaging; CT: computed tomography.

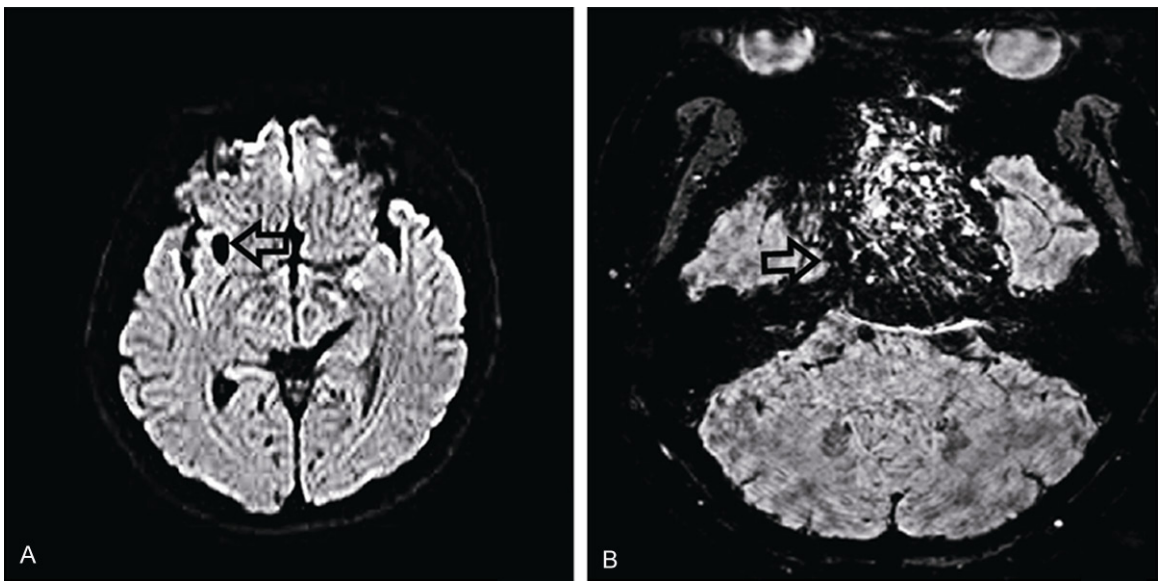

Figure 1. DWI image of hemangioma. A. Right insular lobe hemangioma [b = 1000 s/mm^2, quasi-circular low signal on the right insular lobe]. B. Cavernous sinus region hemangioma [b = 500 s/mm^2, mixing zone of high and low signals could be seen in the cavernous sinus region, and high signals dominated the centre].

image via tissue water displacement, thereby quickly scanning biological tissues comprehensively, and free from ion irradiation [7, 8]. In consequence, MR-DWI is now used frequently in various clinical diagnoses, especially in cancers [9, 10]. Yet computed tomography (CT) adopts X-ray and ultrasound wave to perform profile scanning on part of the human body, and then uses a detector with high sensitivity to collect, which is characterized by high scanning speed and distinct images [11]. According to our study, MR-DWI is more advantageous than CT in clinical diagnosis, especially for cancers. With regard to the imaging degree, unclear

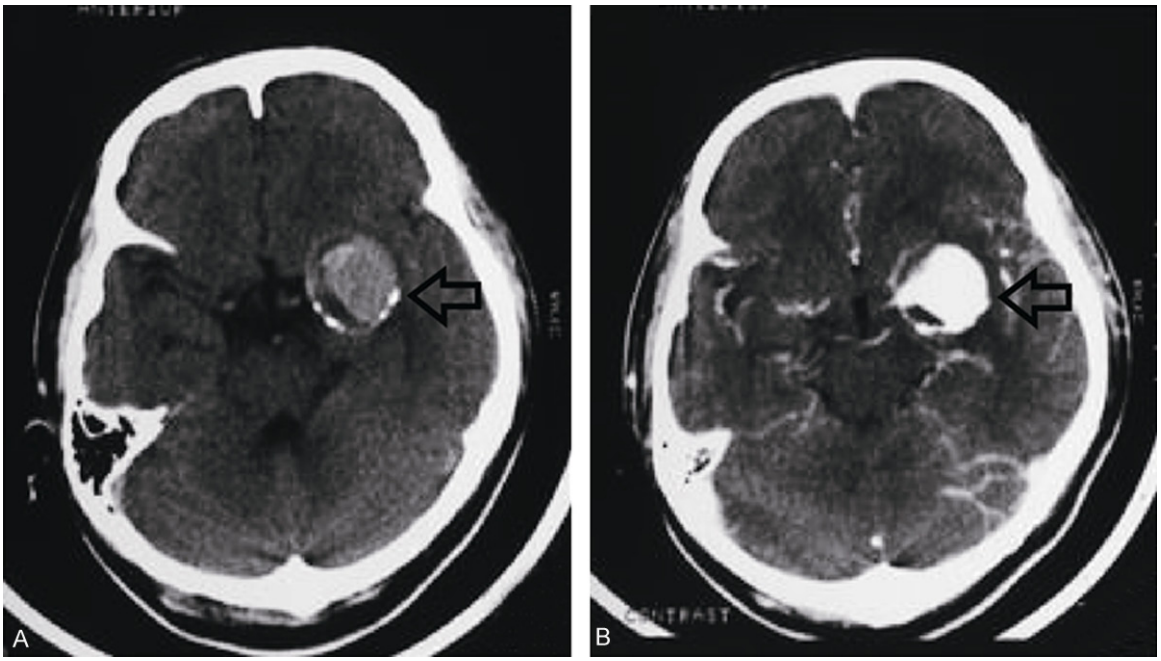

Figure 2. CT image of head basal ganglia aneurysm. A. CT plain scan showed isodensity; B. After CT enhanced scan, focal zone was significantly enhanced.

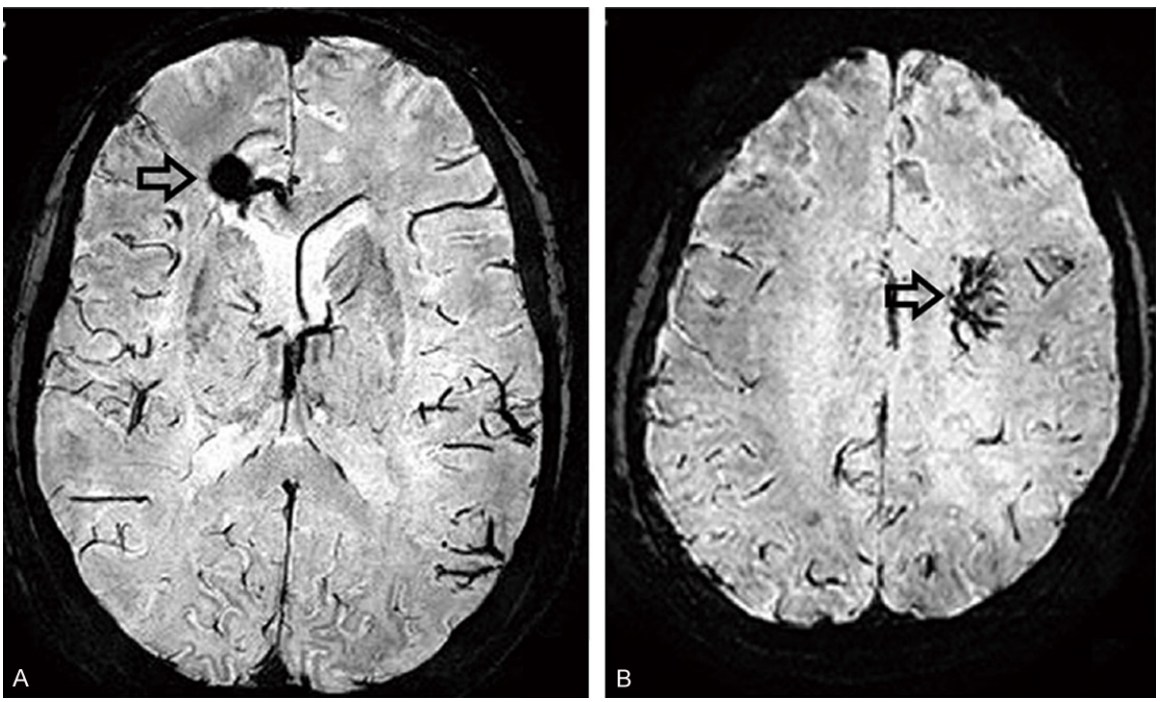

Figure 3. DWI figure of venous malformation. A. Venous malformation in the right frontal lobe [b = 1000 s/mm^2, quasi-circular and strip-shaped low signals in the medullary region of the right frontal lobe]; B. Venous malformation in the left ganglion region [b = 500 s/mm^2, 'caput medusae' signal on the left semi oval center].

imaging may sometimes occur in CT scanning, thus making it difficult to diagnose diseases [12]. Therefore, our study compares CT and MRI in diagnosis effect through conducting CT and MRI imaging diagnosis with hemangioma or venous malformation on the head and neck

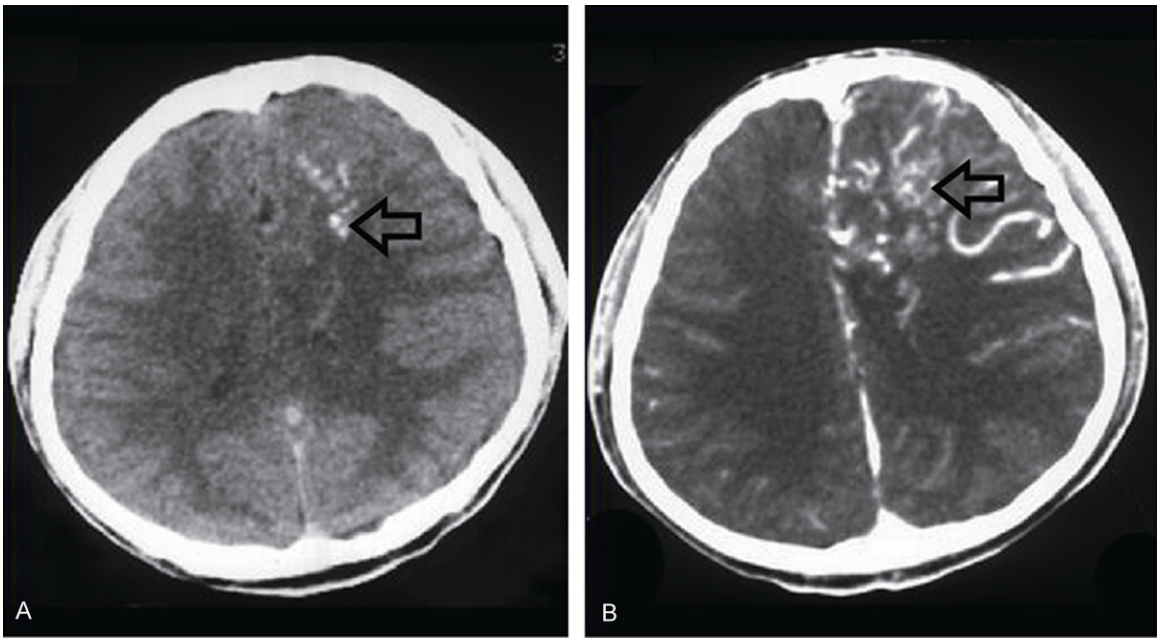

Figure 4. Venous malformation in left frontal lobe of brain. A. CT plain scan showed isodensity; B. Focal zone was slightly enhanced after CT scan enhancement.

among children, and further identifies the diagnostic advantages and value of MR-DWI while diagnosing hemangioma and venous malformation.

Materials and methods

Subjects

During March 2013 and March 2015, a total of 55 children with hemangioma or venous malformation on the head and neck in our hospital were recruited into this study, including 25 cases with hemangioma and 30 cases with venous malformation. Confirmed by surgery and pathology or digital subtraction angiography (DSA), all patients were initially diagnosed as hemangioma or venous malformation on the head and neck. Exclusion criteria were as follows: (1) all patients were clinically diagnosed without performing tissue biopsy before CT and MRI imaging diagnosis; (2) radiotherapy or chemotherapy was not conducted for all subjects; (3) low-quality MRI image caused by human movement and cystic lesion with high ADC value was also excluded [13]. Among all recruited patients, there were 35 men and 20 women, aged from 1 to 18 years old (average age: 11.6). Further, all eligible subjects were examined with MRI and CT. This study has been approved by the ethics committee of our hospital. All included subjects and their parents or guardians were informed of the experiment and have signed the written consent. All procedures in this study were in compliance with the Declaration of Helsinki involving human beings [14].

MRI method

Inspection equipment for patients in both groups was GE 1.5T SIGNA TWINSPEED scanner (GE Healthcare, Milwaukee Wisconsin). All patients were in supine position with their head and neck combined with surface coil, and conventional MRI imaging was adopted. MRI imaging parameters were as follows. (1) Transverse section T2 FRFSE: TE: 85.0 ms; TR: 3700 ms; ETL: 19; bandwidth: 31.25 Hz; FOV: 22V 25 Hz; slice thickness: 3.0 mm; interlayer spacing: 1.0 mm; matrix: 320 mmHz; NEX: 3; and scanning time lasted for 1 min. (2) Transverse section T1 FSE: TE: 11.0 ms; TR: 500 ms; ETL: 3; bandwidth: 31.25 Hz; FOV: 22 cm 5 Hzth; slice thickness: 3.0 mm; interlayer spacing: 1.0 mm; matrix: 320 mm; NEX: 1; and the scanning time lasted for 1 min and 8 s. (3) Coronal section (sagittal section) T2 FRFSE: TE: 85.0 ms; TR: 3825 ms; ETL: 19; bandwidth: 31.25 Hz; FOV: 18 cm: 31.2; slice thickness: 3.0 mm; interlayer spacing: 1.0 mm; matrix: 320 mm; NEX: 2; and the scanning time lasted for 1 min and 32 s. For

Table 2. Comparison of CT, MR-DWI and pathological diagnosis in the diagnosis of hemangioma and venous malformation

Methods		Pathological diagnosis	
		Hemangioma group (case)	Venous malformation group (case)
MR-DWI	Hemangioma group (case)	23	4
	Venous malformation group (case)	2	26
CT	Hemangioma group (case)	21	8
	Venous malformation group (case)	4	22

MR-DWI: magnetic resonance diffusion-weighted imaging; CT: computed tomography.

Table 3. Evaluation of diagnostic efficiency of CT and MR-DWI in hemangioma and venous malformation

Methods	Accuracy	Sensitivity	Specificity	Predictive value of positive diagnosis	Predictive value of negative diagnosis	*Kappa* test	
						K	*P*
MR-DWI	89.10%	92.00%	86.70%	85.2%	92.9%	0.781	0.000
CT	78.20%	84.00%	73.30%	72.4%	84.6%	0.566	0.000

Note: K refers to the matching coefficient in *K*appa test; MR-DWI: magnetic resonance diffusion-weighted imaging; CT: computed tomography.

Table 4. Comparison of mean ADC value between hemangioma patients and venous malformation patients ($^{-3}mm^2/s$)

b value	Hemangioma group (n = 25)	Venous malformation group (n = 30)	*P*
500 s/mm2	1.325 ± 0.309	1.952 ± 0.321	< 0.01
1000 s/mm^2	0.739 ± 0.245	1.215 ± 0.235	< 0.01

MR-DWI imaging, parameters were as follows: values of diffusion coefficient b were set as 500 s/mm^2 and 1000 s/mm^2, respectively. Transverse section was adopted for the single shot of SE-EPI sequence; TR: 2225~4000 ms, TE: 51.8-70 ms, number of excitation: 8, slice thickness: 5 mm, interlayer spacing: 0.5 mm, field of view: 24 cm × 24 cm, matrix: 128 × 128.

CT examination method

Whole-body CT scanner Somatom Plus and Somatom Plus 4 produced by Siemens were applied to conduct the CT plain scan for the cross section of head and neck, with slice thickness of 3~8 mm. And screw pitch was set as 1.0 in spiral scanning. As for CT enhanced scan, spiral CT scanner Light speed-16 manufactured by GE was applied. Scanning parameters were as follows: detector structure of 16 × 1.25 mm mode; coverage 20 cm/r; screw pitch 1.375: 1 (table speed 27.5 mm/r) or 0.938: 1 (table speed 18.75 mm/r); reconstruction thickness 7.5 mm; thinnest thickness of reconstruction 1.25 mm; and injection speed of enhancement scan contrast medium 3.0 ml/s.

Image analysis and measurement

DWI scanning data were imported into ADW 4.4 workstation, and the Function software was adopted to process original images. Selection of region of interest (ROC) was as follows: (1) Taking plain scan and enhanced scan as references, the inclusion of solid part of lesion was maximized, while calcification and bleeding region of lesion was excluded. (2) The largest slice of the solid part of lesion was selected, and the ADC value was the lowest among three measurements. Original CT images were imported to ADW4.4 workstation to post-process image, and techniques, including multiplanar reconstruction (MPR), maximum intencity projection (MIP) and volume rendering (VR) were used to conduct multiplanar reconstruction and three-dimensional volume rendering. Finally, double blind method was adopted to evaluate DWI and CT images by 2 experienced imaging experts. Disagreements were resolved through discussion to reach consensus about evaluation. Sensitivity, specificity, and accuracy of both methods when diagnosing hemangioma and venous malformation were calculated respectively.

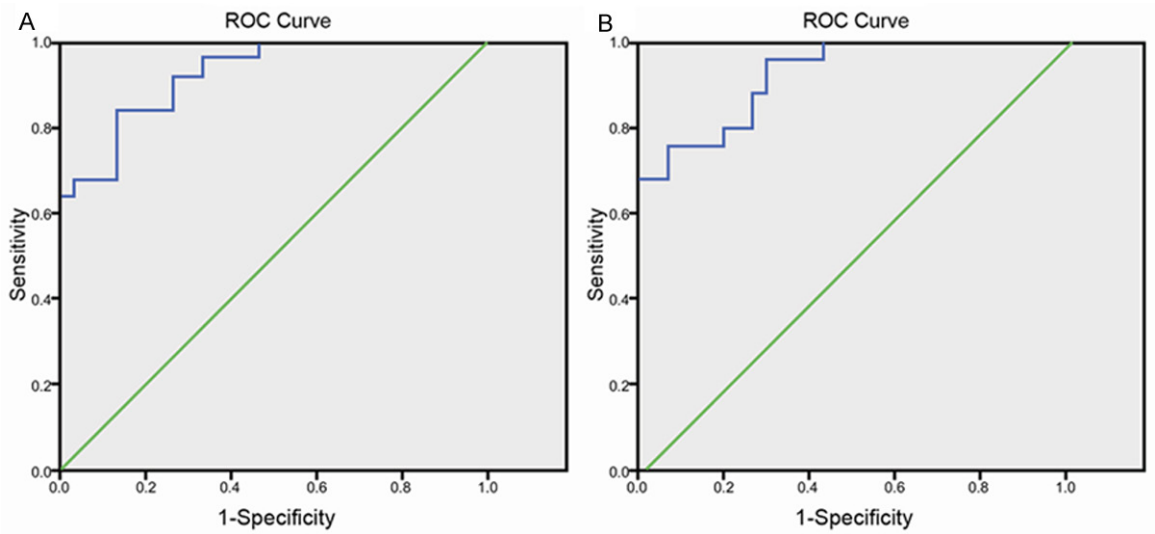

Figure 5. Receiver operating characteristic curve of MR-DWI. A. b = 500 s/mm^2; B. b = 1000 s/mm^2.

Statistical method

Statistical analysis was conducted using SPSS19.0 software (SPSS Inc, Chicago, IL, USA). Continuous measurement data were presented as mean ± standard deviation ($\bar{X}$ ± s) and tested by Student's *t* test; count data were presented with percentage and compared by χ^2 test. χ^2 test and *Kappa* test of count data were adopted for both methods (MR-DWI and CT) and pathology. It was generally acknowledged that $K \geq 0.75$ showed high consistency and matching degree between the two methods; when $0.4 \leq K < 0.7$, the matching degree was moderate; and when $K < 0.4$, the matching degree was low. Accuracy = (true positive + true negative)/(true positive + false negative +false positive + true negative); sensitivity = true positive/(true positive + false negative); specificity = true negative/(true negative + false positive); positive predictive value = true positive/(true positive + false positive); negative predictive value = true negative/(true negative + false negative). Accuracy, sensitivity and specificity of MR-DWI and CT in diagnosing hemangioma and venous malformation were calculated. And ROC curve was drawn to determine the optimal threshold in identifying hemangioma and venous malformation on head and neck. $P < 0.05$ was considered to be statistically significant.

Results

Baseline characteristics of all patients

Baseline characteristics of all recruited 55 patients diagnosed with hemangioma or venous malformation on the head and neck were presented in **Table 1**. Age of patients in the hemangioma group was significantly lower than that in the venous malformation group ($P < 0.05$). No obvious difference was seen between both groups with respect to sex, lesion extent, pathogenic site, color of lesion and treatment means (all $P > 0.05$).

Comparison of MR-DWI and CT images in hemangioma and venous malformation

MR-DWI and CT manifestations of hemangioma were shown as below: on MR-DWI images, all subjects showed high signals (compared with muscle tissue) with irregular shapes, including 20 cases with heterogeneous signals and 5 cases with relatively homogeneous signals; there were also 20 subjects with ill-defined margins and 5 subjects with well-defined margins; (**Figure 1**). On CT plain scan, 17 cases were characterized by isodensity and 8 cases by iso-or-low density, which were heterogeneous. Furthermore, among 4 cases, high-density and dot-shaped phlebolith could be observed. After enhancement scan, 19 sub-

jects showed significant enhancement and 6 subjects show moderate enhancement, and they all had heterogeneous enhancement. Among them, 8 subjects had large worm-like vascular masses inside (**Figure 2**).

MR-DWI and CT findings of venous malformation were shown as below: on MR-DWI images, 6 cases showed intermediate signals and 24 cases showed slightly high signals, which were heterogeneous with divisions inside and irregular shapes. Ill-defined borders were observed seen in 6 cases, and well-defined borders observed in 23 cases (**Figure 3**). Plain scan of lesions displayed 12 subjects with heterogeneous isodensity, 9 subjects with cystic low density, 5 subjects with heterogeneous slightly-high density, and 4 subjects with homogeneous isodensity. And dot-shaped tight phlebolith could be seen in 5 subjects. After enhancement scan, 9 cases experienced heterogeneous enhancement, 11 cases showed no significant enhancement, and 3 cases had divided enhancement (**Figure 4**).

Diagnostic efficiency of MR-DWI and CT

MR-DWI and CT were applied to measure lesion of 55 patients with hemangioma or venous malformation, and results of pathology diagnosis were used as the gold standard to perform data analysis. The result was shown in **Table 2**. Compared with CT, MR-DWI had higher accuracy, sensitivity, specificity, and positive and negative predictive values in the diagnosis of hemangioma and venous malformation. It was found that results of both methods were consistent with results of pathological analysis, and the matching coefficient of MR-DWI (K = 0.781) was significantly higher than that of CT (K = 0.566) (**Table 3**).

ROC curve of MR-DWI

When b = 500 s/mm^2, average ADC values in the hemangioma group and venous malformation group were 1.325 ± 0.309 and 1.952 ± 0.321, respectively. ADC value in the venous malformation group was higher than that in the hemangionma group (P < 0.05) (**Table 4**); area under the ROC curve (AUC) was 0.924, threshold was reached when ADC = 1.615 × 10^{-3} mm^2/s. And sensitivity and specificity for the threshold were 84.00% and 86.70%, respectively (**Figure 5A**). When b value was 1000 s/mm^2, average ADC values in the hemangioma group and venous malformation group were 0.739 ± 0.245 and 1.215 ± 0.235, respectively, and the latter was higher than the former (P < 0.05) (**Table 4**); the AUC was 0.924, and threshold was reached when ADC = 0.894 × 10^{-3} mm^2/s, with sensitivity and specificity of 76.0% and 67.0%, respectively, obviously lower than sensitivity and specificity respectively when b = 500 s/mm^2 (**Figure 5B**).

Discussion

Hemangioma and venous malformation on the head and neck are common diseases among children, MR-DWI and CT scanning are widely used in their diagnosis. According to current reports, result of MR-DWI can be more accurate and valid than CT scan, thus being more suitable for clinical diagnosis [15, 16]. The main purpose of this study was to compare the two common diagnostic methods, MR-DWI and CT, to compare their advantages and estimate actual values of MR-DWI in the diagnosis of hemangioma and venous malformation on the head and neck among children.

It turned out that the scanning results of MR-DWI were more intuitional and interpretable compared with CT, and the former showed higher sensitivity especially in terms of lesions: the results of MR-DWI tended to have rather clear outline and apparent lesion, but results of CT scan were not so clear and CT scan could only use enhancement scan to obtain obvious images. This can be explained by the fact that MR-DWI primarily depends on the dispersion effect of water molecules in detecting tissues in different status. Dispersion in a living tissue is correlated with its spatial structure, so dispersion of water molecules in the tissue may easily be affected by factors such as the distribution of cell membrane and basement membrane, ratio of nucleus to cytoplasm, and the distribution of macromolecular substance in cytoplasm [9, 10, 17, 18]. Therefore, this may lead to significant difference in dispersion coefficient between tumor cells and normal tissues, which is rather apparent on the image; whereas CT scan mainly depends on signals as X-ray to release images, the sensitivity of which is lower [19].

Through comparison with the actual inspection results, it could obviously be seen that accura-

cy of MR-DWI was higher than that of CT. In addition to accuracy and sensitivity, MR-DWI also had higher positive and negative predictive values. As previously mentioned, MR-DWI had higher inspection sensitivity for diseases cases than CT, and thereby could completely obtain lesion images more comprehensively [19]. However, generally speaking, adoption of two methods to diagnose hemangioma and venous malformation, to a large extent, relies on people's understanding of images. Namely, while using CT scan, people may make wrong diagnostic decisions in lack of evidence since difference of normal and lesion tissues on the scanning image cannot be easily distinguished, thereby decreasing the effect of positive and negative prediction; yet MR-DWI can provide accurate diagnostic evidence more effectively in the absence of significantly distinct and clear images, which helps health practitioners make correct diagnostic decision [12, 19]. This is consistent with the result of previous studies on the diagnostic effect of MR-DWI and CT scan [15, 16].

On the other hand, through further analysis, it can be easily seen that image of MR-DWI is more visible and clearer when b value is 500 s/mm^2. In general, lower values of b can produce images with higher signal-to-noise ratio, with low sensitivity to the detection of water molecule dispersion. Accordingly, higher ADC values and lower stability can be reached with lower values of b; indeed, higher signal values lead to lower signal-to-noise ratio. But this will also lead to increased susceptibility artifact and, accordingly, more severe image distortion, which will eventually influence the measurement results [20]. In consequence, a better b value can help keep the dispersion weight of DWI image under proper control, thereby increasing contrast between lesion tissue and normal tissue to help health practitioners have more accurate diagnosis. It is acknowledged that when b > 500 s/mm^2, most measuring errors of DWI and ADC value produced by blood perfusion can be eliminated [21]. Hence, measuring comparison between two levels of b value, 500 s/mm^2 and 800 s/mm^2, was conducted in this experiment. According to the result, it could be obviously seen that higher sensitivity of MR-DWI for both hemangioma and venous malformation would be achieved when b = 500 s/mm^2. So it can be inferred that diffusion of water molecules is rather apparent among hemangioma and venous malformation, and detection with higher b value will make images more unstable. Therefore, it is more suitable to set the b value as 500 s/mm^2 in diagnosing both diseases.

In conclusion, compared with traditional CT scan, MR-DWI is more sensitive and accurate, which can help health practitioners diagnose hemangioma and venous malformation more effectively. Moreover, if the b value is set accurately, higher sensitivity and specificity of MR-DWI can be seen, thus being valuable in the early diagnosis of hemangioma and venous malformation among children.

Acknowledgements

We would like to acknowledge the helpful comments on this paper received from our reviewers.

Disclosure of conflict of interest

None.

Address correspondence to: Dr. Shoujiang Wang, Department of Medical Imaging, Linyi Peoples Hospital Affiliated to Shandong University, Jiefang Road No. 27, Lanshan Area, Linyi 276003, P. R. China. Tel: +86-0539-8216094; E-mail: wangshoujiang91@163.com

References

[1] Phung TL and Hochman M. Pathogenesis of infantile hemangioma. Facial Plast Surg 2012; 28: 554-562.

[2] Lo K, Mihm M and Fay A. Current theories on the pathogenesis of infantile hemangioma. Semin Ophthalmol 2009; 24: 172-177.

[3] Atherton DJ. Infantile haemangiomas. Early Hum Dev 2006; 82: 789-795.

[4] Wong A, Hardy KL, Kitajewski AM, Shawber CJ, Kitajewski JK and Wu JK. Propranolol accelerates adipogenesis in hemangioma stem cells and causes apoptosis of hemangioma endothelial cells. Plast Reconstr Surg 2012; 130: 1012-1021.

[5] Richter GT and Friedman AB. Hemangiomas and vascular malformations: Current theory and management. Int J Pediatr 2012; 2012: 645678.

[6] Mohr JP, Parides MK, Stapf C, Moquete E, Moy CS, Overbey JR, Al-Shahi Salman R, Vicaut E, Young WL, Houdart E, Cordonnier C, Stefani

MA, Hartmann A, von Kummer R, Biondi A, Berkefeld J, Klijn CJ, Harkness K, Libman R, Barreau X, Moskowitz AJ and international Ai. Medical management with or without interventional therapy for unruptured brain arteriovenous malformations (aruba): A multicentre, non-blinded, randomised trial. Lancet 2014; 383: 614-621.

[7] Nougaret S, Tirumani SH, Addley H, Pandey H, Sala E and Reinhold C. Pearls and pitfalls in mri of gynecologic malignancy with diffusion-weighted technique. AJR Am J Roentgenol 2013; 200: 261-276.

[8] Sala E, Rockall A, Rangarajan D and Kubik-Huch RA. The role of dynamic contrast-enhanced and diffusion weighted magnetic resonance imaging in the female pelvis. Eur J Radiol 2010; 76: 367-385.

[9] Thoeny HC, Forstner R and De Keyzer F. Genitourinary applications of diffusion-weighted mr imaging in the pelvis. Radiology 2012; 263: 326-342.

[10] Rosenkrantz AB, Mussi TC, Melamed J, Taneja SS and Huang WC. Bladder cancer: Utility of mri in detection of occult muscle-invasive disease. Acta Radiol 2012; 53: 695-699.

[11] Sagara Y, Hara AK, Pavlicek W, Silva AC, Paden RG and Wu Q. Abdominal ct: Comparison of low-dose ct with adaptive statistical iterative reconstruction and routine-dose ct with filtered back projection in 53 patients. AJR Am J Roentgenol 2010; 195: 713-719.

[12] Liyanage SH, Roberts CA and Rockall AG. Mri and pet scans for primary staging and detection of cervical cancer recurrence. Womens Health (Lond Engl) 2010; 6: 251-267; quiz 268-259.

[13] Razek A, Nada N, Ghaniem M and Elkhamary S. Assessment of soft tissue tumours of the extremities with diffusion echoplanar mr imaging. Radiol Med 2012; 117: 96-101.

[14] M PN. World medical association publishes the revised declaration of helsinki. Natl Med J India 2014; 27: 56.

[15] Blomqvist L. Preoperative staging of colorectal cancer--computed tomography and magnetic resonance imaging. Scand J Surg 2003; 92: 35-43.

[16] Tondo F, Saponaro A, Stecco A, Lombardi M, Casadio C and Carriero A. Role of diffusion-weighted imaging in the differential diagnosis of benign and malignant lesions of the chest-mediastinum. Radiol Med 2011; 116: 720-733.

[17] Wang HJ, Pui MH, Guo Y, Yang D, Pan BT and Zhou XH. Diffusion-weighted mri in bladder carcinoma: The differentiation between tumor recurrence and benign changes after resection. Abdom Imaging 2014; 39: 135-141.

[18] Avcu S, Koseoglu MN, Ceylan K, Bulut MD and Unal O. The value of diffusion-weighted mri in the diagnosis of malignant and benign urinary bladder lesions. Br J Radiol 2011; 84: 875-882.

[19] Siegel R, Naishadham D and Jemal A. Cancer statistics, 2013. CA Cancer J Clin 2013; 63: 11-30.

[20] Koike N, Cho A, Nasu K, Seto K, Nagaya S, Ohshima Y and Ohkohchi N. Role of diffusion-weighted magnetic resonance imaging in the differential diagnosis of focal hepatic lesions. World J Gastroenterol 2009; 15: 5805-5812.

[21] Padhani AR, Liu G, Koh DM, Chenevert TL, Thoeny HC, Takahara T, Dzik-Jurasz A, Ross BD, Van Cauteren M, Collins D, Hammoud DA, Rustin GJ, Taouli B and Choyke PL. Diffusion-weighted magnetic resonance imaging as a cancer biomarker: Consensus and recommendations. Neoplasia 2009; 11: 102-125.